Stem Cell Reports
Report

ISSCR

OPEN ACCESS

Recapitulation of Clinical Individual Susceptibility to Drug-Induced QT Prolongation in Healthy Subjects Using iPSC-Derived Cardiomyocytes

Tadahiro Shinozawa,[1,*] Koki Nakamura,[2] Masanobu Shoji,[3] Maya Morita,[1] Maya Kimura,[1] Hatsue Furukawa,[1] Hiroki Ueda,[5] Masanari Shiramoto,[6] Kyoko Matsuguma,[7] Yoshikazu Kaji,[8] Ippei Ikushima,[8] Makoto Yono,[9] Shyh-Yuh Liou,[5] Hirofumi Nagai,[1] Atsushi Nakanishi,[3] Keiji Yamamoto,[3] and Seigo Izumo[4]

[1]Drug Safety Research Laboratories, Pharmaceutical Research Division, Takeda Pharmaceutical Company Limited, 26-1 Muraoka-Higashi 2-chome, Fujisawa, Kanagawa 251-8555, Japan
[2]Global Medical Affairs-Japan, Takeda Pharmaceutical Company Limited, 12-10 Nihonbashi 2-chome, Chuo-ku, Tokyo 103-8668, Japan
[3]Integrated Technology Research Laboratories
[4]Regenerative Medicine Unit
Pharmaceutical Research Division, Takeda Pharmaceutical Company Limited, 26-1 Muraoka-Higashi 2-chome, Fujisawa, Kanagawa 251-8555, Japan
[5]Development Operations Department, Takeda Development Center Japan, Pharmaceutical Development Division, Takeda Pharmaceutical Company Limited, 12-10 Nihonbashi 2-chome, Chuo-ku, Tokyo 103-8668, Japan
[6]Hakata Clinic, Souseikai, 6-18 Tenya-machi, Hakata-ku, Fukuoka 812-0025, Japan
[7]Sugioka Memorial Hospital (current Fukuoka Mirai Hospital), Souseikai, 5-1 Kashii-Teriha 3-chome, Higashi-ku, Fukuoka 813-0017, Japan
[8]Sumida Hospital, Souseikai, 1-29-1 Honjo, Sumida-ku, Tokyo 130-0004, Japan
[9]Nishi-Kumamoto Hospital, Souseikai, 1012 Koga, Tomiai-machi, Minami-ku, Kumamoto 861-4157, Japan
*Correspondence: tadahiro.shinozawa@takeda.com
http://dx.doi.org/10.1016/j.stemcr.2016.12.014

SUMMARY

To predict drug-induced serious adverse events (SAE) in clinical trials, a model using a panel of cells derived from human induced pluripotent stem cells (hiPSCs) of individuals with different susceptibilities could facilitate major advancements in translational research in terms of safety and pharmaco-economics. However, it is unclear whether hiPSC-derived cells can recapitulate interindividual differences in drug-induced SAE susceptibility in populations not having genetic disorders such as healthy subjects. Here, we evaluated individual differences in SAE susceptibility based on an in vitro model using hiPSC-derived cardiomyocytes (hiPSC-CMs) as a pilot study. hiPSCs were generated from blood samples of ten healthy volunteers with different susceptibilities to moxifloxacin (Mox)-induced QT prolongation. Different Mox-induced field potential duration (FPD) prolongation values were observed in the hiPSC-CMs from each individual. Interestingly, the QT interval was significantly positively correlated with FPD at clinically relevant concentrations ($r > 0.66$) in multiple analyses including concentration-QT analysis. Genomic analysis showed no interindividual significant differences in known target-binding sites for Mox and other drugs such as the hERG channel subunit, and baseline QT ranges were normal. The results suggest that hiPSC-CMs from healthy subjects recapitulate susceptibility to Mox-induced QT prolongation and provide proof of concept for in vitro preclinical trials.

INTRODUCTION

Serious adverse events (SAE) are major causes of drug attrition during clinical development (Hay et al., 2014) or withdrawal of marketed drugs. Although models for nonclinical toxicology and safety pharmacological studies have improved in recent years, predicting SAE in preclinical studies remains challenging because SAE often occur in a small SEA-prone patient subgroup (Stevens and Baker, 2009). Moreover, conventional cellular or animal models are not suitable for the investigation of interindividual differences in drug susceptibility. Interestingly, cardiomyocytes derived from human induced pluripotent stem cells (hiPSC-CMs; Takahashi et al., 2007) can be used to assess disease-associated genetic susceptibility to drug-induced cardiac toxicity in vitro (Liang et al., 2013). hiPSC-CMs from individuals with different susceptibilities to SAE have been proposed to serve as a novel translational research model for in vitro preclinical trials (Inoue et al., 2014). However, whether or not individual SAE susceptibility in a population of volunteers with unknown genetic susceptibility such as healthy volunteers can be recapitulated in hiPSC-derived cells remains unclear. Generally, in phase I studies healthy volunteers are recruited to assess the toxicity and drug distribution in the body under low dosing and, in many clinical trials, genetic background-associated drug susceptibility to SAE is unknown before dosing. Therefore, it is important to assess the intrinsic drug susceptibility before dosing to prevent side effects.

Here, we tested this concept using healthy volunteer-derived hiPSC-CMs, which have contractile ability with ion channel activity and have been recognized for their potential in human heart disease modeling, preclinical cardiotoxicity evaluation, and drug discovery (Zhang et al., 2009). Drug-induced torsades de pointes (TdP) is the most common reason for market restriction or withdrawal of drugs (Lasser et al., 2002). TdP is typically caused by inhibition of the inward rectifying potassium channel hERG (human ether-à-go-go related gene encoded by *KCNH2*), resulting in a prolongation of the time between

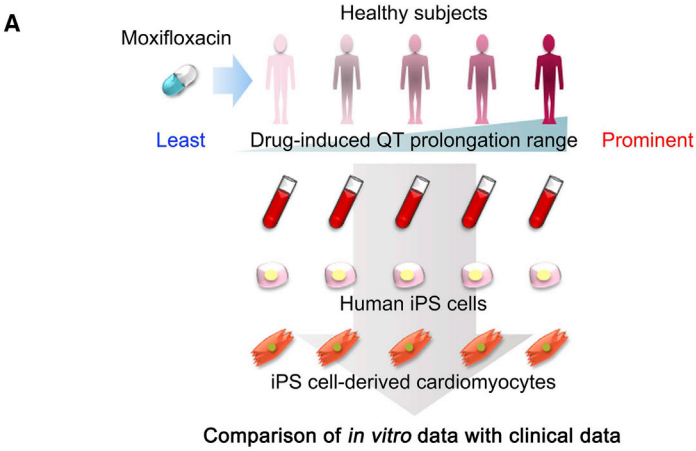

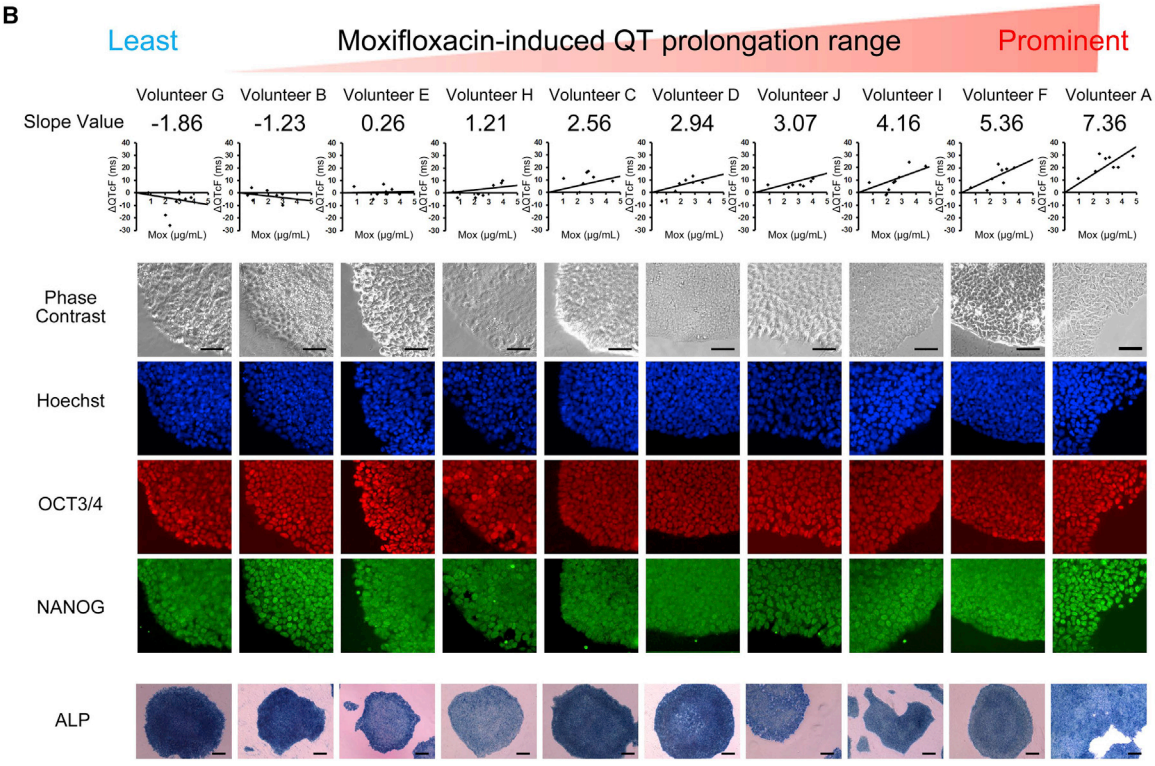

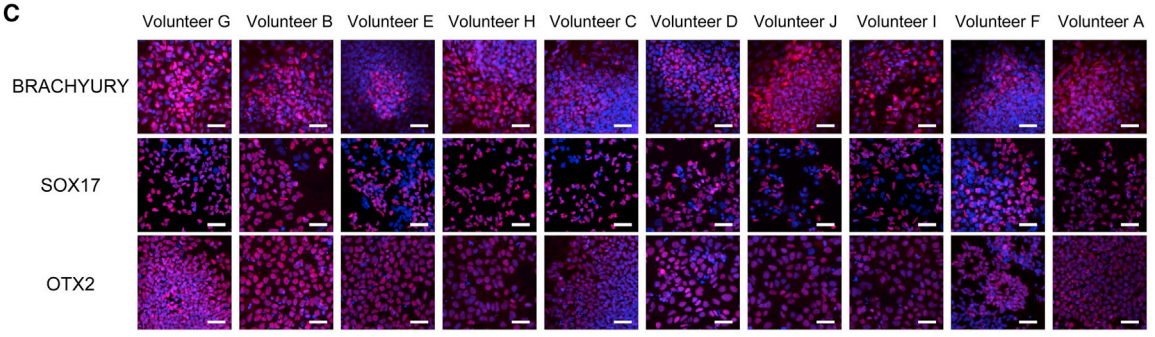

(legend on next page)

depolarization and repolarization, known as the QT interval (Guo et al., 2011). hiPSC-CMs are a useful tool for the assessment of drug-induced QT prolongation (Sallam et al., 2015; Mehta et al., 2011; Reppel et al., 2005; Braam et al., 2010). Thus, we evaluated the correlation between susceptibility to moxifloxacin (Mox)-induced QT prolongation (Chen et al., 2005; Roden, 2004; Sherazi et al., 2008) and that to Mox-induced prolonged repolarization in hiPSC-CMs generated from blood samples of the same individuals from our previous clinical investigational study, in which we observed interindividual susceptibility to QT prolongation (Shiramoto et al., 2014). Mox, a fluoroquinolone antibiotic and a rapid delayed-rectifier potassium channel blocker that prolongs QT, is commonly used as a positive control in "thorough QT" (TQT) studies (Chen et al., 2005; Florian et al., 2011). These are designed to measure QT prolongation to better assess the potential arrhythmia liability of a drug in healthy volunteers based on the regulatory guidelines for new drug development (Food and Drug Administration, HHS, 2005).

RESULTS

Generation of hiPSCs from Peripheral Blood of Healthy Volunteers

hiPSCs were generated from blood samples of ten healthy male volunteers with different sensitivities to Mox-induced QT prolongation (Figure 1; Tables S1 and S2), ranging from baseline (ΔQTcF) to placebo-adjusted prolonged ranges from baseline (ΔΔQTcF), calculated using the Fridericia correction: QTcF = QT/RR(1/3) (Fridericia, 1920). The degree of sensitivity was defined using slope values of ΔQTcF or ΔΔQTcF, calculated with the Mox plasma concentration before and at eight time points after dosing in a concentration-QT analysis (Figure 1B) (Garnett et al., 2008). To reprogram blood cells, we used Sendai virus (SeV)-encoded Yamanaka 4 factors as described by Seki et al. (2010). Alkaline phosphatase, OCT3/4, and NANOG stained positively, and stem cell-related genes were upregulated in all blood cell-derived hiPSCs (Figure 1B and Table S3). In addition, markers of the three germ layers, BRACHYURY, SOX17, and OTX2, stained positively in mesoderm, endoderm, and ectoderm derived from hiPSCs, respectively (Figure 1C).

Differentiation of hiPSCs into Cardiomyocytes In Vitro

Differentiation of hiPSCs into cardiomyocytes was induced using embryoid body (EB) differentiation after approximately 20 passages. After 30–50 days of differentiation, hiPSC-CMs stained positive for cardiac-specific markers, GATA4, cardiac actin, and cardiac troponin T (Figure 2A). More than 85% of hiPSC-CMs were cardiac actin-positive cells (Figures 2B and 2C). Genes related to muscle development were upregulated in hiPSC-CMs (Table S3). Although expression analysis showed that the hiPSC-CMs were distinct from adult ventricular tissue (Figure S1A) and the expression of the muscle contraction genes *MYH6* and *RYR2* was lower than that in adult ventricular tissue, the overall gene expression related to muscle contraction and ion channel activity in hiPSC-CMs was closer to that in adult ventricular tissue (Figures 2D, 2E, and S1B). In addition, hierarchical clustering based on genes related to cardiac contractility showed that hiPSC-CMs derived from each participant were categorized in the same cluster including adult ventricular tissue (Figure 2E). Some genes were differentially expressed in hiPSC-CMs. The correlation between individual expression and in vivo slope value data was analyzed. In almost all genes related to cardiac contractility, no significant correlation was observed. Although a significant negative correlation was observed in one probe of *AKAP9* ($r = -0.64$), no correlation with other probes of *AKAP9* was observed. Therefore, it was difficult to consider the contribution of *AKAP9* gene expression to the correlation.

Field Potential Duration in iPSC-CMs

hiPSC-CMs spontaneously contracted in a microelectrode array (MEA) (Figures 3A and 3B, Movie S1). Susceptibility to Mox-induced prolongation of repolarization was confirmed by measuring the field potential duration (FPD) (Figure 3B), a reference widely used to correlate QT prolongation with clinical outcomes (Sallam et al., 2015; Mehta et al., 2011; Reppel et al., 2005; Braam et al., 2010). Clear peaks existed in all FPD data, and MEA measurements were performed properly; FPD cannot be determined when the amplitude is greatly reduced or shows bimodality, e.g., in the presence of a drug. Moreover, because the beating rate of the hiPSC-CMs (mean 40 beats/min, $n = 125$) was lower than that in humans and did not show large changes over

Figure 1. Study Outline and Profiling of Human iPSCs Derived from Blood Samples of Each Volunteer

(A) Schematic representation of the experimental approach.

(B) Representative slopes of ΔQTcF with the plasma concentration of moxifloxacin (Mox) and immunostaining for OCT3/4 (red) and NANOG (green) in iPSCs. Nuclei were counterstained with Hoechst 33342 (blue). Scale bars, 50 μm. The bottom panel (scale bars, 200 μm) shows alkaline phosphatase (ALP) staining of iPSC colonies.

(C) Immunostaining for BRACHYURY (red), SOX17 (red), and OTX2 (red) in iPSC-derived mesoderm, endoderm, and ectoderm, respectively. Nuclei were counterstained with Hoechst 33342 (blue). Scale bars, 50 μm.

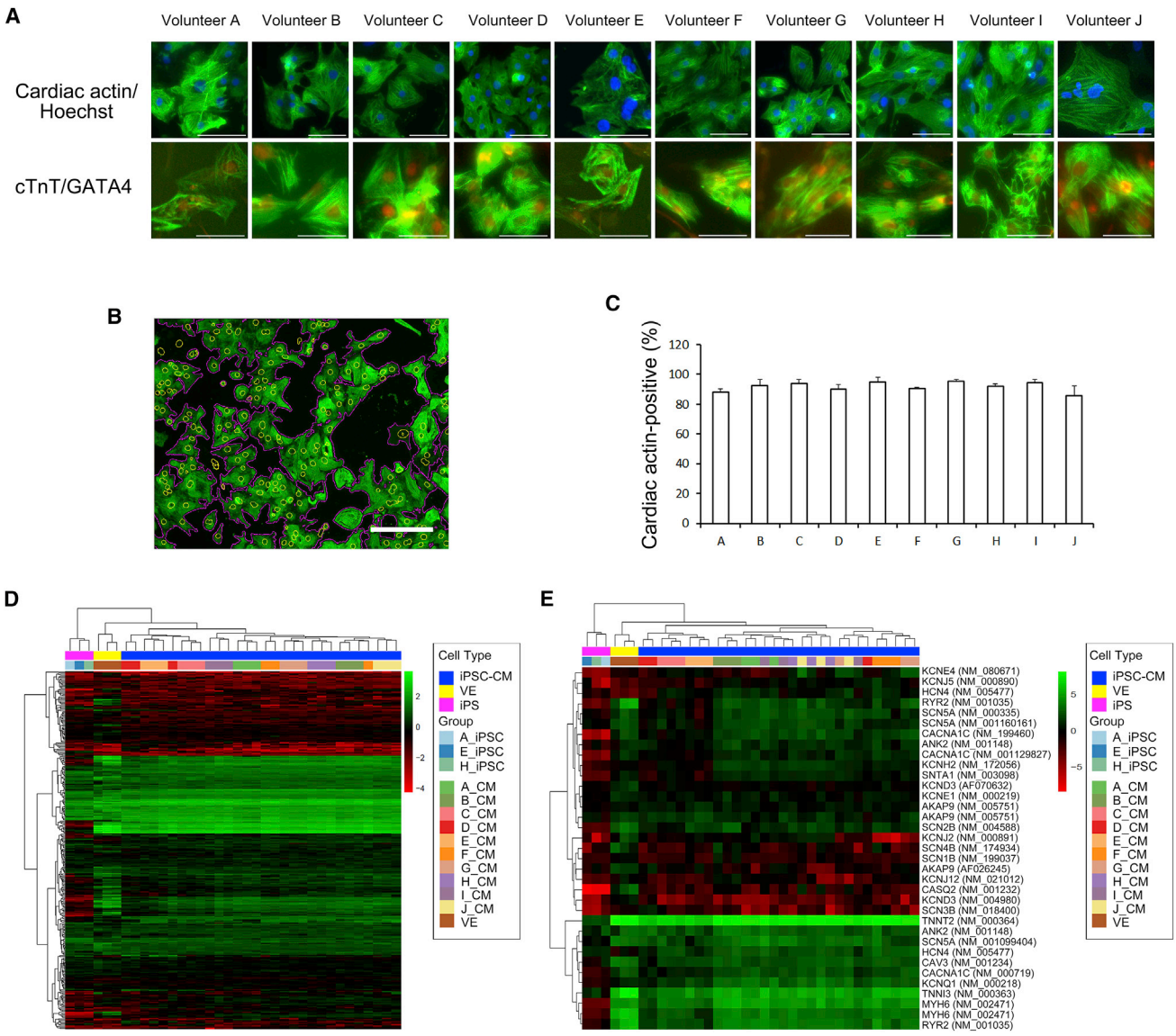

Figure 2. Profiling of hiPSC-Derived Cardiomyocytes from Healthy Participants

(A) Immunostaining for cardiac actin (green), cardiac troponin T (cTnT, green), and GATA4 (red) in iPSC-derived cardiomyocytes (iPSC-CMs). Nuclei were counterstained with Hoechst 33342 (blue). Scale bars, 50 μm.

(B and C) iPSC-derived cardiomyocytes isolated from beating cell clusters. (B) Detection of cardiac actin-positive cells using an IN Cell Analyzer 1000. Scale bar, 200 μm. (C) Average ratio of cardiac actin-positive to total cells in hiPSC-derived beating cell clusters. A–J show the study subjects. Error bars represent the mean ± SEM of the independent experiments (n = 3–9).

(D and E) Hierarchical cluster analysis of gene expression in hiPSC-CMs with undifferentiated iPSCs and adult ventricular tissue. (D) Heatmap of genes (241 genes, 331 probes) categorized as regulating muscle contraction (GO: 6937) and having voltage-gated ion channel activity (GO: 5244). (E) Heatmap of genes related to cardiac contractile function. VE, adult ventricular tissue; A–J_CM, hiPSC-CMs derived from each volunteer.

various concentrations of Mox in some hiPSC-CM lines (Figure S2A), correction for beating rate was not applied to avoid excessive correction. Different slopes of FPD prolongation were obtained for different doses of Mox in each individual (Figure 3C), depending on the Mox concentration range (Figure 3D). The timing of hiPSC-CM differentiation was not correlated with the extent of FPD change for all Mox concentrations tested (Figure 3E).

Relationship between In Vivo and In Vitro Data

We evaluated whether or not the susceptibility to FPD prolongation in hiPSC-CMs reflected that to QT prolongation

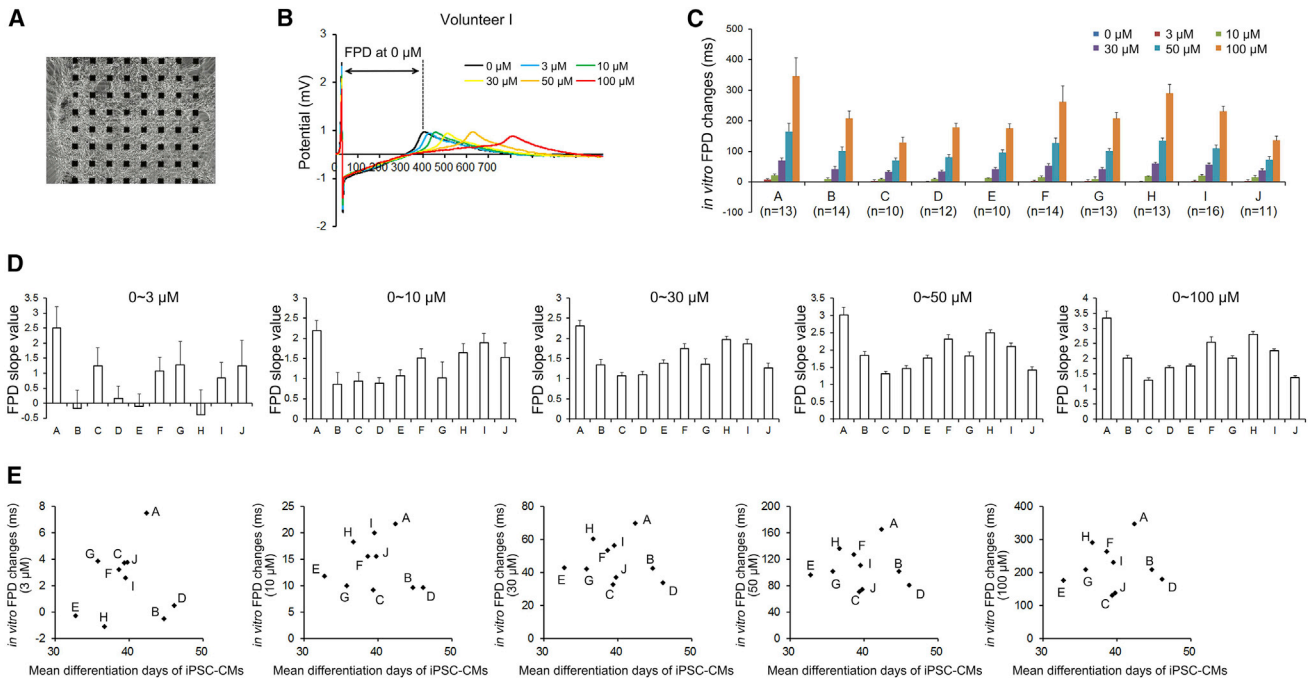

Figure 3. Prolongation of Mox-Induced Field Potential Duration in iPSC-CMs from Each Participant

(A) Phase-contrast image of iPSC-CMs plated onto a multielectrode chamber.

(B) Representative waveforms of field potential recorded after dosing with Mox (0, 3, 10, 30, 50, and 100 μM).

(C) Changes in field potential duration (FPD) induced by Mox (0, 3, 10, 30, 50, and 100 μM) in iPSC-CMs from all volunteers. Error bars represent the mean ± SEM of the independent experiments (n = 10–16).

(D) Slopes of FPD for the indicated concentrations of Mox in iPSC-CMs from each individual. Error bars represent the mean ± SEM of the independent experiments (n = 10–16).

(E) Relationship between timing of differentiation (days) and FPD in hiPSC-CMs from all volunteers.

in vivo. Because the susceptibility of subjects was evaluated based on the slopes of ΔQTcF or ΔΔQTcF defined according to Mox concentration based on the concentration-response relationship, in vivo and in vitro susceptibility was compared using the FPD slope value calculated with the Mox concentration based on concentration-response relationship. Surprisingly, FPD prolongation slopes at 0–10 μM Mox, but not at 0–3 μM and >30 μM Mox, in hiPSC-CMs were significantly and positively correlated with those of ΔQTcF ($r = 0.73$, $p = 0.016$) and ΔΔQTcF ($r = 0.66$, $p = 0.036$) (Figures 4A–4C; Table S4). FPD slope values were also compared with QT prolongation values at maximum plasma exposure (maximum plasma concentration, C_{max}). Significant positive correlations ($r = 0.64$–0.85) of slope values at 0–3 μM and/or 0–10 μM Mox in hiPSC-CMs were observed with ΔQTcF-C_{max} or ΔΔQTcF-C_{max} (Figures 4D–4F and Table S4).

Genetic Analysis of Representative Drug-Binding Sequences in *KCNH2*

The possible relationship between individual susceptibility to Mox-induced QT prolongation and genetic mutations were investigated by genome sequence analysis in chromosome NC_000007.13 encoding T623, S624, V625, G648, Y652, and F656, which are known to alter sensitivity to Mox and drugs when mutated (Mitcheson et al., 2000; Alexandrou et al., 2006). Only a TAT/TAC synonymous substitution was found in the codon for Y652 in all individuals (four heterozygotes, six homozygotes) (Table S5).

Analysis of SNPs Associated with Drug-Induced TdP

To investigate the possible relationship between individual susceptibility to drug-induced TdP and mutations, we searched for SNPs in 53 genes reported to be associated with drug-induced TdP in NCBI and a previous genome-wide association study (GWAS) (Behr et al., 2013) using an Infinium Human Exome Bead Chip (Illumina). One polymorphism (rs81204) with minor allele frequency (MAF) 0.2238 in *KCNQ1* was found in volunteers F and A, who showed the highest susceptibility to Mox (Table S6). No differences in the polymorphisms rs4799838 at *RPRD1A* and rs9805984 and rs1014001 at *FRMD6*, which were reported to significantly associate with drug-induced TdP in the GWAS (Behr et al., 2013), were observed among

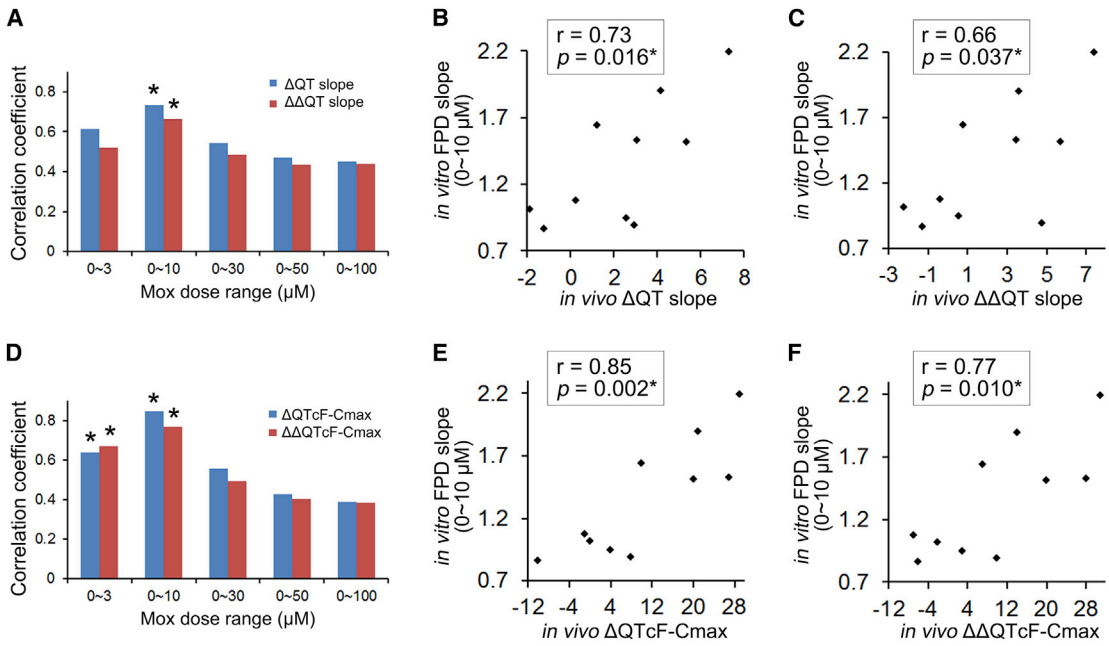

Figure 4. Correlation between In Vivo and In Vitro Data

(A) Correlation coefficient between in vitro FPD slope for the indicated Mox concentrations from each participant and ΔQTcF (blue) and ΔΔQTcF (red) slopes. *p < 0.05.

(B and C) Correlation between in vitro FPD slope from each participant at 0–10 μM Mox, and ΔQTcF (B) and ΔΔQTcF (C) slopes for the same individual.

(D) Correlation coefficient between in vitro FPD slope for the indicated Mox concentrations from each participant and ΔQTcF-C_{max} (blue) and ΔΔQTcF-C_{max} (red) slopes. *p < 0.05.

(E and F) Correlation between in vitro FPD slope from each participant at 0–10 μM Mox, and ΔQTcF-C_{max} (E) and ΔΔQTcF-C_{max} (F) slopes for the same individual.

volunteers having different susceptibilities to Mox. However, five SNPs (rs2238092, rs216013, rs21615, rs1076390, and re98545) in *CACNA1C* related to cLQTS8, three SNPs (rs6683160, rs1362841, and rs10802592) in *RYR2* related to drug-induced QT prolongation (Kääb et al., 2012; Ramirez et al., 2013), and three SNPs (rs17707180, rs11132322, and rs10022111) in *PALLD* reportedly related to antipsychotic drugs (olanzapine, perphenazine, quetiapine, risperidone, and ziprasidone) inducing QT prolongation (Aberg et al., 2012), showed differences between volunteers with low (G, B, E, and H) and high (I, F, A) Mox susceptibility (Table S6 and Figure 1B).

DISCUSSION

We demonstrated a significant positive correlation between the susceptibility of hiPSC-CMs to Mox-induced FPD prolongation and QT prolongation in healthy individuals within a certain concentration range. Thus, in vitro assays using hiPSCs derived from healthy individuals may improve cardiotoxicity risk assessment in drug development. The combination with assay models to assess genetic susceptibility (Liang et al., 2013) would further enhance the prediction of SAE occurring in small subgroups. Despite the small study cohort (n = 10), the data were considered reliable because the correlations in individuals were highly consistent across different parameters and all measurements were obtained in a blinded manner. It will be necessary to evaluate the practical usability of this system in a large-scale clinical study including a large number of volunteers.

An MEA was used to investigate the relationship between in vivo electrocardiography (ECG) data and in vitro data in iPSC-CMs because the synchronous beating of a cultured cardiac myocyte monolayer in vitro shows electric patterns similar to those of the heart. Moreover, MEAs may be most useful when used not only to evaluate the electrophysiological properties of cardiomyocytes but also to correlate them with tissue networks (Sallam et al., 2015). However, one major concern related to MEA is that the data depend on the filtering of the signal from cells, and FPD cannot be determined in case of absent or bimodal field potential peaks. To address these concerns, we only measured FPDs including high peaks. Thus, we considered the use of an

MEA for a cell sheet appropriate for comparison with ECG QT intervals. The slope values of Mox-induced FPD prolongation were affected by Mox concentration, and significant positive correlations were observed at Mox concentrations of 0–10 μM. Similar results were observed in comparison with QT prolongation values at C_{max}. The maximum Mox plasma concentration was 3.01–5.35 mg/L (6–11 μM) (Table S1), and Mox is known to have a low protein-binding rate (approximately 40%) (Stass and Kubitza, 1999). In addition, it has been reported that electrophysiological properties and drug responses of human embryonic stem cell-derived cardiomyocytes match clinical observations on QT prolongation at similar concentrations (Braam et al., 2010), suggesting that the concentrations that yielded significant positive correlations in vitro were in the range of plasma exposure in the clinical study. The non-significant correlation at concentrations >30 μM in vitro might be explained by off-target effects at supra-pharmacological concentrations. We observed a significant positive correlation at Mox concentrations of 0–3 μM for ΔQTcF-C_{max} and ΔΔQTcF-C_{max}, but not for ΔQTcF-slope and ΔΔQTcF-slope; one of the reasons may be the different algorithm used to quantify susceptibility in vivo. ΔQTcF- and ΔΔQTcF-slope values were affected by hysteresis, which is a delay in equilibration between plasma concentrations and QT changes. In fact, the range for QT prolongation was larger at later than at earlier time points at the same plasma Mox concentration in some individuals, indicating counterclockwise hysteresis (Figure S2B). In addition, we observed variability in the data at 0–3 μM (Figure 3E). For a more accurate correlation it will be necessary to reduce the noise in the in vitro measurement.

We could not investigate detailed cellular mechanisms to explain the correlation between in vivo and in vitro data because of unavailability of heart tissue samples from each participant; therefore, we investigated the possible role of genetic variation. hiPSC-CMs with specific mutations have phenotypes that are similar to the disease phenotype, including long QT syndrome (Liang et al., 2013; Itzhaki et al., 2011). However, the participants had no genetic mutations that would result in amino acid changes in target-binding sites for Mox or other drugs associated with the induction of QT prolongation. Moreover, the baseline QT ranges were normal (410 ± 14 ms) (Burke et al., 1997) in the study participants. Although some genes such as *KCNE4* and *KCNH2* were differentially expressed among hiPSC-CM lines, these differences did not correlate with in vivo data. In SNP analysis only one polymorphism, (rs81204) in *KCNQ1*, was present in two volunteers highly susceptible to Mox. On the other hand, we could not confirm a correlation with a polymorphism in *FRMD6* reported in a GWAS (Behr et al., 2013) in our volunteers. Interestingly, five SNPs in *CACNA1C* related to cLQTS8 and three SNPs in *RYR2* related to drug-induced QT prolongation (Kääb et al., 2012; Ramirez et al., 2013) were different between volunteers with low and high susceptibility to Mox. On the other hand, three SNPs in *PALLD* related to antipsychotic drug-induced QT prolongation (Aberg et al., 2012) showed differences between volunteers with low and high susceptibility. This might be explained by the fact that these are different types of drugs. Interestingly, the frequency of these three SNPs differs between Japanese (MAF 0.1–0.2) and Europeans (MAF 0.4–0.5). Although the relationship between this polymorphism and phenotypes was difficult to determine because of the small cohort, these SNPs might be one of the candidates to indicate evidence in the relationship of different susceptibility between in vivo and hiPSC-CMs. Further GWASs using a larger number of participants with diverse polymorphisms are warranted. The hiPSC-CM model has some limitations (Denning et al., 2016), such as the immature phenotype (Zhu et al., 2014) or indeterminate subtypes of cardiomyocytes (David and Franz, 2012). However, they are useful for high-throughput plate assays and high-content imaging (Mercola et al., 2013) because there is no contamination with other cell types (Burridge et al., 2016). In addition, extension of the culture period induces maturation in hiPSC-CMs (Yang et al., 2014). Therefore, the immature features and gap in differentiation periods among hiPSC-CMs derived from an individual might limit the recapitulation of drug susceptibility to Mox between a subject and hiPSC-CMs derived from the subject. To obtain a high correlation score between human susceptibility and hiPSC-CMs, it is necessary to improve the differentiation method to prepare more mature cardiomyocytes and control their different maturation states.

In the present study, we demonstrated the potential of hiPSC-CMs to reflect an adverse drug response in healthy individuals. However, as mentioned above, studies in larger cohorts of individuals and using various types of drugs will be required to translate this potential into practical applications. Recently, the revision of the TQT study regulatory guidelines (the International Conference on Harmonization E14 guidelines) has been the subject of discussion because of substantial costs and limited accuracy (Food and Drug Administration, HHS, 2005; Chi, 2013). We believe our data provide an insight that can be expected to greatly contribute to the current discussion. We anticipate that our results will be highly valuable for minimizing cardiac risks associated with drug development in humans.

EXPERIMENTAL PROCEDURES

Generation of hiPSCs from Blood Samples

hiPSCs were generated from blood cells as described previously (Seki et al., 2010). Peripheral blood mononuclear cells (PBMCs) were isolated from heparinized whole-blood samples using a

Ficoll gradient. T cell proliferation in the PBMCs was stimulated using interleukin-2 (IL-2)-supplemented medium (TaKaRa Bio) and anti-CD3 monoclonal antibody (BD Pharmingen) bound to the plate. At approximately day 5 of culture, Sendai virus vectors (CytoTune-iPS For Blood Cells; DNAVEC) encoding human OCT3/4, SOX2, KLF4, and c-MYC were used to infect T cells at an MOI of 20 according to the manufacturer's protocol. Twenty-four hours after infection, the medium was replaced with fresh IL-2-supplemented medium. The next day, Sendai virus-infected PBMCs were plated on a feeder layer of mitomycin-C-treated mouse embryonic fibroblasts in Primate ES medium (ReproCELL) supplemented with 4 ng/mL recombinant human basic fibroblast growth factor (Peprotech) in an atmosphere of 5% CO_2/95% air. Approximately 15 days after transduction, hiPSC colonies emerged and were transferred onto another plate. We verified the absence of SeV in all iPSCs used in this study after passage 12 by using a TaqMan iPSC Sendai Detection Kit (Invitrogen). To confirm the differentiation into the three germ layers, we differentiated all human iPSCs into mesoderm, endoderm, and ectoderm, and stained for the markers BRACHYURY, SOX17, and OTX2, respectively, using the Human Pluripotent Stem Cell Functional Identification Kit (R&D Systems) according the manufacturer's instructions.

In this study, all subjects provided written informed consent before participating, and the protocol was approved by the institutional review boards of Takeda Pharmaceutical Company Limited and Kyushu Clinical Pharmacology Research Clinic in Fukuoka, Japan.

ACCESSION NUMBERS

Microarray data deposited in the GEO database can be accessed with the accession number GEO: GSE92391.

SUPPLEMENTAL INFORMATION

Supplemental Information includes Supplemental Experimental Procedures, two figures, six tables, and one movie and can be found with this article online at http://dx.doi.org/10.1016/j.stemcr.2016.12.014.

AUTHOR CONTRIBUTIONS

T.S. designed the study, performed and analyzed experiments, and wrote the manuscript. K.N. designed the study, analyzed the data, and wrote the manuscript. M.S. generated iPSCs and analyzed the microarray data. M.M. measured FPD in iPSC-derived cardiomyocytes. M.K. and H.F. performed the differentiation of iPSCs into cardiomyocytes. H.U., M.S., K.M., Y.K., I.I., and M.Y. performed the clinical studies. S.-Y.L. analyzed genotyping. H.N., A.N., K.Y., and S.I. designed the study, analyzed data, and wrote the manuscript.

ACKNOWLEDGMENTS

We thank Dr. Atsushi Sugiyama of the Department of Pharmacology, School of Medicine, Toho University, for insightful discussion and advice; Dr. Takanori Takebe of the Department of Pediatrics, Cincinnati Children's Hospital Medical Center, for insightful advice; Kazuaki Enya, Kazuhiko Asari, Mikiko Nii, Aya Mishima, and Mariko Nakaike of Takeda Pharmaceutical Company Ltd. for assistance with the clinical study; Dr. Kenichi Nagatome, Dr. Teruaki Okuda, Yoshiko Okai, and Yoshiyuki Furukawa of Drug Safety Research Laboratories, Takeda Pharmaceutical Company Ltd.; Hiroshi Sawada of Pharmaceutical Research Division, Takeda Pharmaceutical Company Ltd., for helpful suggestions; Hiroko Akiyama and Tomohiro Kotaki of Takeda Pharmaceutical Company Ltd. for technical assistance; and Dr. Fumiyo Saito of Chemicals Evaluation and Research Institute for assistance with microarray study. This work was funded by Takeda Pharmaceutical Company.

Received: May 14, 2016
Revised: December 14, 2016
Accepted: December 15, 2016
Published: January 19, 2017

REFERENCES

Aberg, K., Adkins, D.E., Liu, Y., McClay, J.L., Bukszár, J., Jia, P., Zhao, Z., Perkins, D., Stroup, T.S., Lieberman, J.A., Sullivan, P.F., and van den Oord, E.J. (2012). Genome-wide association study of antipsychotic-induced QTc interval prolongation. Pharmacogenomics J. *12*, 165–172.

Alexandrou, A.J., Duncan, R.S., Sullivan, A., Hancox, J.C., Leishman, D.J., Witchel, H.J., and Leaney, J.L. (2006). Mechanism of herg K^+ channel blockade by the fluoroquinolone antibiotic moxifloxacin. Br. J. Pharmacol. *147*, 905–916.

Behr, E.R., Ritchie, M.D., Tanaka, T., Kääb, S., Crawford, D.C., Nicoletti, P., Floratos, A., Sinner, M.F., Kannankeril, P.J., Wilde, A.A., et al. (2013). Genome wide analysis of drug-induced torsades de pointes: lack of common variants with large effect sizes. PLoS One *8*, e78511.

Braam, S.R., Tertoolen, L., van de Stolpe, A., Meyer, T., Passier, R., and Mummery, C.L. (2010). Prediction of drug-induced cardiotoxicity using human embryonic stem cell-derived cardiomyocytes. Stem Cell Res. *4*, 107–116.

Burke, J.H., Ehlert, F.A., Kruse, J.T., Parker, M.A., Goldberger, J.J., and Kadish, A.H. (1997). Gender-specific differences in the QT interval and the effect of autonomic tone and menstrual cycle in healthy adults. Am. J. Cardiol. *79*, 178–181.

Burridge, P.W., Li, Y.F., Matsa, E., Wu, H., Ong, S.G., Sharma, A., Holmström, A., Chang, A.C., Coronado, M.J., Ebert, A.D., Knowles, J.W., Telli, M.L., Witteles, R.M., Blau, H.M., Bernstein, D., Altman, R.B., and Wu, J.C. (2016). Human induced pluripotent stem cell-derived cardiomyocytes recapitulate the predilection of breast cancer patients to doxorubicin-induced cardiotoxicity. Nat. Med. *22*, 547–556.

Chen, X., Cass, J.D., Bradley, J.A., Dahm, C.M., Sun, Z., Kadyszewski, E., Engwall, M.J., and Zhou, J. (2005). QT prolongation and proarrhythmia by moxifloxacin: concordance of preclinical models in relation to clinical outcome. Br. J. Pharmacol. *146*, 792–799.

Chi, K.R. (2013). Revolution dawning in cardiotoxicity testing. Nat. Rev. Drug Discov. *12*, 565–567.

David, R., and Franz, W.M. (2012). From pluripotency to distinct cardiomyocyte subtypes. Physiology (Bethesda) *27*, 119–129.

Denning, C., Borgdorff, V., Crutchley, J., Firth, K.S., George, V., Kalra, S., Kondrashov, A., Hoang, M.D., Mosqueira, D., Patel, A.,

Prodanov, L., Rajamohan, D., Skarnes, W.C., Smith, J.G., and Young, L.E. (2016). Cardiomyocytes from human pluripotent stem cells: from laboratory curiosity to industrial biomedical platform. Biochim. Biophys. Acta *1863*, 1728–1748.

Florian, J.A., Tornøe, C.W., Brundage, R., Parekh, A., and Garnett, C.E. (2011). Population pharmacokinetic and concentration—QTc models for moxifloxacin: pooled analysis of 20 thorough QT studies. J. Clin. Pharmacol. *51*, 1152–1162.

Food and Drug Administration, HHS. (2005). International Conference on Harmonisation: guidance on E14 clinical evaluation of QT/QTc interval prolongation and proarrhythmic potential for non-antiarrhythmic drugs; availability. Notice. Fed. Regist. *70*, 61134–61135.

Fridericia, L.S. (1920). The duration of systole in the electrocardiogram of normal subjects and of patients with heart disease. Acta Med. Scand. *53*, 469–486.

Garnett, C.E., Beasley, N., Bhattaram, V.A., Jadhav, P.R., Madabushi, R., Stockbridge, N., Tornoe, C.W., Wang, Y., Zhu, H., and Gobburu, J.V. (2008). Concentration-QT relationships play a key role in the evaluation of proarrhythmic risk during regulatory review. J. Clin. Pharmacol. *48*, 13–18.

Guo, L., Abrams, R.M., Babiarz, J.E., Cohen, J.D., Kameoka, S., Sanders, M.J., Chiao, E., and Kolaja, K.L. (2011). Estimating the risk of drug-induced proarrhythmia using human induced pluripotent stem cell-derived cardiomyocytes. Toxicol. Sci. *123*, 281–289.

Hay, M., Thomas, D.W., Craighead, J.L., Economides, C., and Rosenthal, J. (2014). Clinical development success rates for investigational drugs. Nat. Biotechnol. *32*, 40–51.

Inoue, H., Nagata, N., Kurokawa, H., and Yamanaka, S. (2014). iPS cells: a game changer for future medicine. EMBO J. *33*, 409–417.

Itzhaki, I., Maizels, L., Huber, I., Zwi-Dantsis, L., Caspi, O., Winterstern, A., Feldman, O., Gepstein, A., Arbel, G., Hammerman, H., et al. (2011). Modelling the long QT syndrome with induced pluripotent stem cells. Nature *471*, 225–229.

Kääb, S., Crawford, D.C., Sinner, M.F., Behr, E.R., Kannankeril, P.J., Wilde, A.A., Bezzina, C.R., Schulze-Bahr, E., Guicheney, P., Bishopric, N.H., et al. (2012). A large candidate gene survey identifies the KCNE1 D85N polymorphism as a possible modulator of drug-induced torsades de pointes. Circ. Cardiovasc. Genet. *5*, 91–99.

Lasser, K.E., Allen, P.D., Woolhandler, S.J., Himmelstein, D.U., Wolfe, S.M., and Bor, D.H. (2002). Timing of new black box warnings and withdrawals for prescription medications. JAMA *287*, 2215–2220.

Liang, P., Lan, F., Lee, A.S., Gong, T., Sanchez-Freire, V., Wang, Y., Diecke, S., Sallam, K., Knowles, J.W., Wang, P.J., et al. (2013). Drug screening using a library of human induced pluripotent stem cell-derived cardiomyocytes reveals disease-specific patterns of cardiotoxicity. Circulation *127*, 1677–1691.

Mehta, A., Chung, Y.Y., Ng, A., Iskandar, F., Atan, S., Wei, H., Dusting, G., Sun, W., Wong, P., and Shim, W. (2011). Pharmacological response of human cardiomyocytes derived from virus-free induced pluripotent stem cells. Cardiovasc. Res. *91*, 577–586.

Mercola, M., Colas, A., and Willems, E. (2013). Induced pluripotent stem cells in cardiovascular drug discovery. Circ. Res. *112*, 534–548.

Mitcheson, J.S., Chen, J., Lin, M., Culberson, C., and Sanguinetti, M.C. (2000). A structural basis for drug-induced long QT syndrome. Proc. Natl. Acad. Sci. USA *97*, 12329–12333.

Ramirez, A.H., Shaffer, C.M., Delaney, J.T., Sexton, D.P., Levy, S.E., Rieder, M.J., Nickerson, D.A., George, A.L., Jr., and Roden, D.M. (2013). Novel rare variants in congenital cardiac arrhythmia genes are frequent in drug-induced torsades de pointes. Pharmacogenomics J. *13*, 325–329.

Reppel, M., Pillekamp, F., Brockmeier, K., Matzkies, M., Bekcioglu, A., Lipke, T., Nguemo, F., Bonnemeier, H., and Hescheler, J. (2005). The electrocardiogram of human embryonic stem cell-derived cardiomyocytes. J. Electrocardiol. *38*, 166–170.

Roden, D.M. (2004). Drug-induced prolongation of the QT interval. N. Engl. J. Med. *350*, 1013–1022.

Sallam, K., Li, Y., Sager, P.T., Houser, S.R., and Wu, J.C. (2015). Finding the rhythm of sudden cardiac death: new opportunities using induced pluripotent stem cell-derived cardiomyocytes. Circ. Res. *116*, 1989–2004.

Seki, T., Yuasa, S., Oda, M., Egashira, T., Yae, K., Kusumoto, D., Nakata, H., Tohyama, S., Hashimoto, H., Kodaira, M., et al. (2010). Generation of induced pluripotent stem cells from human terminally differentiated circulating T cells. Cell Stem Cell *7*, 11–14.

Sherazi, S., DiSalle, M., Daubert, J.P., and Shah, A.H. (2008). Moxifloxacin-induced torsades de pointes. Cardiol. J. *15*, 71–73.

Shiramoto, M., Uchimaru, H., Kaji, Y., Matsuguma, K., Matsuki, S., Ikushima, I., Yonou, M., and Irie, S. (2014). Evaluation of assay sensitivity and the concentration-effect relationship of moxifloxacin in a QT/QTc study in Japan. Ther. Innov. Regul. Sci. *48*, 181–189.

Stass, H., and Kubitza, D. (1999). Pharmacokinetics and elimination of moxifloxacin after oral and intravenous administration in man. J. Antimicrob. Chemother. *43* (*Suppl B*), 83–90.

Stevens, J.L., and Baker, T.K. (2009). The future of drug safety testing: expanding the view and narrowing the focus. Drug Discov. Today *14*, 162–167.

Takahashi, K., Tanabe, K., Ohnuki, M., Narita, M., Ichisaka, T., Tomoda, K., and Yamanaka, S. (2007). Induction of pluripotent stem cells from adult human fibroblasts by defined factors. Cell *131*, 861–872.

Yang, X., Pabon, L., and Murry, C.E. (2014). Engineering adolescence: maturation of human pluripotent stem cell-derived cardiomyocytes. Circ. Res. *114*, 511–523.

Zhang, J., Wilson, G.F., Soerens, A.G., Koonce, C.H., Yu, J., Palecek, S.P., Thomson, J.A., and Kamp, T.J. (2009). Functional cardiomyocytes derived from human induced pluripotent stem cells. Circ. Res. *104*, e30–e41.

Zhu, R., Blazeski, A., Poon, E., Costa, K.D., Tung, L., and Boheler, K.R. (2014). Physical developmental cues for the maturation of human pluripotent stem cell-derived cardiomyocytes. Stem Cell Res. Ther. *5*, 117.